Title

A Dual-Probe Heat-Pulse Sensor with Rigid Probes for Improved Soil Water Content Measurement

Permalink

Journal

ISSN

Authors

Kamai, Tamir
Kluitenberg, Gerard J
Hopmans, Jan W

Publication Date

DOI

Peer reviewed

A Dual-Probe Heat-Pulse Sensor with Rigid Probes for Improved Soil Water Content Measurement

Tamir Kamai*

Institute of Soil, Water and
Environmental Sciences
Agricultural Research Organization
Volcani Center
Bet Dagan
Israel

Gerard J. Kluitenberg

Dep. of Agronomy
Kansas State Univ.
Manhattan, KS 66506

Jan W. Hopmans

Dep. of Land, Air and Water Resources
Univ. of California
Davis, CA 95616

The dual-probe heat-pulse (DPHP) method is attractive for measuring soil thermal properties and volumetric water content. The purpose of this study was to develop and test a DPHP sensor having rigid probes made from thick-walled stainless steel tubing (2.38-mm outside diameter). The probes of this sensor are much more resistant to deflection than those of conventional DPHP sensors, decreasing measurement error caused by probe deflection during insertion into the soil. Laboratory experiments were conducted across a wide range of saturation levels with glass beads and three soils of different textures. For inferring soil properties from the proposed sensor, we applied the recently developed identical cylindrical perfect conductors (ICPC) model instead of the infinite line source (ILS) model that is typically used. The ICPC model improves solution for heat transport through the probe–soil system by accounting for the heat capacity and radius of the probes. Our results show a root mean square error of 1.4% volumetric water content and elimination of the measurement bias typically encountered with DPHP measurements. We conclude that the improved sensor, in combination with the ICPC model, provides a general, soil-independent water content estimate that is especially suitable for field soil water content monitoring because of its robust design with rigid probes. Because of its simplicity and measurements independent of soil type, we propose the presented DPHP method as an excellent alternative to other available measurement techniques for soil water content.

Abbreviations: DPHP, dual-probe heat-pulse; ICPC, identical cylindrical perfect conductors; ILS, infinite line source.

The dual-probe heat-pulse (DPHP) method is attractive for in situ measurement of soil thermal properties and volumetric water content because the combined soil properties are determined collectively through simple relationships that typically do not require soil-specific calibration (Basinger et al., 2003). The method is implemented with a sensor that has two parallel probes: a heater probe and a temperature probe. A short-duration heat pulse is introduced by the heater probe, and the soil's thermal response is measured a known distance away with the temperature probe. The thermal properties (volumetric heat capacity, thermal conductivity, and thermal diffusivity) are determined by fitting a heat transfer model to the temperature response data (Bristow et al., 1994a). For variably saturated porous media, the volumetric water content can be estimated from the bulk soil volumetric heat capacity using a simple linear fraction mixing model (Bristow et al., 1993; Kluitenberg, 2002) if the soil bulk density and the specific heat of the soil solid constituents are known.

Among the key factors that determine the accuracy of the DPHP method is the capability of the selected soil heat transfer model and associated model parameters to represent the DPHP sensor measurement. The model most commonly used is the infinite line source (ILS) solution of Bristow et al. (1994a), which as-

sumes that heat is conducted from an infinitely long line heat source into a homogeneous, isotropic medium of infinite extent. In practice, however, the sensor's probes are finite in diameter, finite in length, and have thermal properties that differ from those of the soil (Knight et al., 2012). The probes are typically constructed from stainless steel tubing that houses the active electronic components of the probes: a resistant heater wire for the heater probe and a thermistor or thermocouple for the temperature probe. The inside of the tubing is filled with thermally conductive epoxy that holds these electronic components in place and provides thermal contact with the stainless steel tubing. The probes are held parallel by the sensor body, which also serves to house the electronic connections. Because the sensor body is usually made from plastic resin or cast epoxy, its thermal properties also differ from those of the soil.

The original DPHP sensor of Campbell et al. (1991) had stainless steel probes with an inner diameter (id) and an outer diameter (od) of 0.514 and 0.819 mm, respectively (Table 1). Numerous investigators have used this original sensor design to evaluate the DPHP method for quantifying thermal properties and water content (Bilskie et al., 1998; Bristow, 1998; Bristow et al., 1993, 1994a, 1994b; Welch et al., 1996). To improve probe rigidity and help maintain a fixed probe spacing when inserting the sensor into soil, Tarara and Ham (1997) designed sensors with probes that were larger in diameter and had greater wall thickness, with id = 0.838 mm and od = 1.27 mm (Table 1). Sensors with these probe dimensions and with 6-mm probe spacing have been used extensively in both laboratory and field investigations (Basinger et al., 2003; Campbell et al., 2002; Heitman et al., 2003; Ochsner and Baker, 2008; Ochsner et al., 2001, 2003, 2005; Kluitenberg et al., 2010; Song et al., 1998, 1999, 2000). We refer to sensors with these probe dimensions as the conventional DPHP (C-DPHP) sensor (Table 1). It is important to recognize the compromise made in the C-DPHP sensor design between probe rigidity and the need to keep the influence of the probes insignificant for the ILS model. In order for the ILS model to adequately represent the soil–sensor system, the probes of the DPHP sensor need to be long and have a small diameter relative to the distance between the probes. Although probe rigidity was improved in the C-DPHP sensor by increasing the thickness of the stainless steel wall, we note that other approaches have been introduced to minimize the effects caused by probe flexibility. These include sensors with shorter probes or

a larger probe diameter (Ham and Benson, 2004; Kamai et al., 2008, 2010; Mori et al., 2003) and sensors having different probe geometries (Kamai et al., 2009; Olmanson and Ochsner, 2008).

A typical procedure in the DPHP method is to calibrate for probe spacing, thereby introducing an effective distance between the heat source and the temperature response location in the ILS model, lumping the combined effects of the sensor properties into a single model parameter. However, probe-spacing calibration does not eliminate disparities between the ILS model and the DPHP sensor. The results of Ham and Benson (2004) clearly showed that the effective probe spacing depends on the thermal properties of the calibration medium and various sensor properties.

Although the dimensions of the original DPHP sensor were confirmed to be appropriate for the ILS model by Kluitenberg et al. (1993, 1995), their analysis did not account for the thermal properties of the probes. Furthermore, before the work of Knight et al. (2012), the influence of the dimensions and thermal properties of the probes of the C-DPHP sensor had not been thoroughly analyzed. Data obtained with C-DPHP sensors show consistent disparities between measured and actual thermal properties. Specifically, while the measured volumetric heat capacity and water content are well estimated for saturated soil conditions, they are overestimated for dry soil conditions, with a typical linear estimation response for intermediate water contents (Basinger et al., 2003; Heitman et al., 2003; Ochsner et al., 2003; Ren et al., 2003; Tarara and Ham, 1997). In some studies, such as that of Basinger et al. (2003), where considerable attention was given to keeping the probe spacing constant, the DPHP sensor showed similar disparities for a wide range of soil types. Their comparison of DPHP-measured and gravimetrically evaluated volumetric water content showed a linear response with an average offset and slope of 4.1% and 0.92, respectively, for a wide range of soil types and water contents.

Errors in DPHP-measured soil properties certainly can be caused by deflection of the probes during insertion into the soil, even for the more rigid probes of the C-DPHP sensor. However, we attribute the observed bias and offset in volumetric heat capacity and water content mainly to the presence of the probes. Considering that the ILS model does not account for the probes and the sensor body, it cannot fully represent the DPHP sensor because it neglects the contribution of the sensor components to heat transfer in the sensor–soil system (Knight et al., 2012). Knight et al. (2012) hypothesized that the major contributing properties for these disparities are the finite radius and finite heat capacity of the probes, such that the probes can be simulated as infinitely long rods with infinite thermal conductivity and finite heat capacity. They introduced the semi-analytical identical cylindrical perfect conductors (ICPC) solution, proposing it instead of the ILS model for more adequate representation of the DPHP sensor and the sensor–soil system.

The objective of this study was to evaluate rigid DPHP (R-DPHP) sensors in combina-

Table 1. Dimensions of the stainless steel tubing for the original dual-probe heat-pulse (DPHP) sensor of Campbell et al. (1991) and the sensor of Tarara and Ham (1997), which we refer to as the conventional DPHP sensor. Also given are tubing dimensions for the proposed rigid DPHP sensor.

Sensor type	Diameter		Wall thickness	Length	Cross-sectional area
	Inner	Outer			
	mm				mm^2
Original DPHP†	0.514	0.819	0.153	28	0.320
Conventional DPHP	0.838	1.27	0.216	28	0.715
Rigid DPHP	0.959	2.38	0.711	35–45	3.731

† Diameters are for no. 21 hypodermic needles (Medical Tube Technology).

tion with the ICPC model. The R-DPHP sensor has large-diameter, thick-walled stainless steel probes, with id = 0.965 and od = 2.38 mm (Table 1). The increase in probe rigidity achieved with this sensor design was quantified by using solutions of the Euler–Bernoulli equation for beam deflection. The effect of probe length on rigidity was also addressed in this analysis. Two experiments were conducted to evaluate sensor performance. In the first, the optimal probe length was determined by evaluating R-DPHP sensors with different probe lengths. Measurements were also made with C-DPHP sensors, and the results were evaluated using both the ILS and ICPC models to confirm the theoretical findings of Knight et al. (2012). The second experiment focused exclusively on evaluation of the ICPC model in conjunction with the R-DPHP sensor that was determined to have probes of optimal length. The capability of the proposed R-DPHP method to measure the soil water content was evaluated by conducting measurements in glass beads and in three soils with different textures across a wide range of saturation levels. The advantage of the proposed method was also demonstrated by comparing the R-DPHP results with those obtained with the C-DPHP. This study also clarifies issues known for the DPHP methodology when using the ILS model with the C-DPHP sensor, presenting additional advantages for using the proposed method.

MATERIALS AND METHODS
Sensor Construction and Data Acquisition

Four types of DPHP sensors were constructed, each having different probe dimensions and probe spacings (Table 2). Three replicates of each type were made, for a total of 12 sensors. While only one type had probes with dimensions similar to those of the C-DPHP sensor, the other three types (R-DPHP-35, R-DPHP-40, and R-DPHP-45) had rigid probes of varying lengths (Table 2). The materials used for sensor construction (Table 3) were similar to those used by Tarara and Ham (1997). One notable exception is that the probes were filled with silver epoxy (Table 3) having a thermal conductivity 2.5 times greater than that of the epoxy they used (Omegabond 101). Cured samples of both epoxies (three replicates each) were submitted to the Thermophysical Properties Research Laboratory (West Lafayette, IN) for thermal conductivity measurement. The mean conductivity was determined to be 1.04 and 0.43 W m^{-1} K^{-1} for the silver and Omegabond 101 epoxies, respectively, with <10% variation among replicates. The benefit of using the silver

Table 3. Parts and materials used for construction of the dual-probe heat-pulse sensors.

Part	Description	Manufacturer
Heater wire	enameled Nichrome 80 alloy, 79-μm diam., 207.9 Ω m^{-1} resistance	Pelican Wire Company
Thermistor	BetaTHERM Model 10K3MCD1, 10-kΩ resistance at 25 ± 0.2°C	Measurement Specialties
Probe tubing	welded and drawn 304 stainless steel	McMaster-Carr
Thermally conductive epoxy	slow-cure silver epoxy	Arctic Silver
Potting epoxy	2-Ton Epoxy, clear	ITW Devcon

epoxy is that it increases the thermal conductivity of the probes. The construction process was similar for all sensor types, following a procedure like that described by Ham and Benson (2004). The probes were held parallel by the sensor body (Fig. 1), which was cast with potting epoxy (Table 3) and also served to secure all connections between the probes and electrical cables. All heater probes were constructed with four strands (two loops) of enamel-coated resistance wire (Table 3). Because of differences in probe length, the total heater element resistance varied among the sensor types. Resistors were added in the circuitry so that all sensor types received approximately the same current.

The data acquisition system consisted of a datalogger (Model CR3000, Campbell Scientific) for measurement and control, a multiplexer (Model AM16/32B, Campbell Scientific) for signal transmission of thermistors, and a relay controller (Model SDM-CD16AC, Campbell Scientific) for distributing the current to the 12 sensors. An individual direct-current regulated power supply (Tenma Model 72-6628, MCM Electronics) was used for driving the heater-circuit current. Additional key

Fig. 1. The rigid dual-probe heat-pulse (R-DPHP) sensor, with probes that are 2.38 mm in diameter and 40 mm in length (R-DPHP-40), after excavation of the Yolo silt loam at a volumetric water content of 0.23 m^3 m^{-3}.

Table 2. Probe dimensions and probe spacing for the conventional dual-probe heat-pulse (C-DPHP) sensor and the rigid DPHP (R-DPHP) sensors used in this study. The length of the probes is given for the part that is outside the sensor body (and perturbs the soil). Probe spacing is the center-to-center distance between the heater and the temperature probe.

Sensor type	Outer diameter	Length	Spacing
		mm	
C-DPHP	1.27	28	6
R-DPHP-35	2.38	35	7
R-DPHP-40	2.38	40	7
R-DPHP-45	2.38	45	7

elements for the circuitry included a 5-kΩ precision resistor ($\pm$0.01% tolerance, S102 series, Vishay Inc.) for the four-wire half-bridge thermistor circuit and a 1-Ω power shunt ($\pm$0.02% tolerance, Model PLV7, Precision Resistor Company) for current measurement during heating. As typically used for DPHP measurements, we applied a heat pulse of 8-s duration with a heat intensity of about 150 W m^{-1}. Temperatures were recorded at 0.5-s intervals for a duration of 180 s.

Experimental Porous Media, Setup, and Procedures

Four porous media were used (Table 4): glass beads, Tottori sand, Columbia sandy loam, and Yolo silt loam. The soil materials were dried, ground, and passed through a 2-mm sieve. Samples of the four porous media were submitted to the Thermophysical Properties Research Laboratory for specific heat determination by differential scanning calorimetry. The specific heat (three replicates per sample) was determined for the temperature range of 23 to 80°C. Mean specific heat capacities at 23°C (Table 4) and bulk densities were used to determine volumetric heat capacities and subsequently to calculate the volumetric water content with the DPHP method. Apart from specific heat values, soil properties were not analyzed for this study. The glass beads had a mean diameter of 0.5 mm (0.4–0.6 mm diameter range), as reported by the manufacturer. Samples of Tottori sand, Columbia sandy loam, and Yolo silt loam were collected from locations near those used in the studies of Toride et al. (2003), Chen et al. (1999), and Eching et al. (1994), respectively. For reference, particle size data from those studies are provided in Table 4.

Before the measurements in porous media, two types of probe spacing were determined: physical probe spacing, L_{PHY}, and effective probe spacing, L_{EFF}. Physical spacing was measured with a digital caliper ($\pm$0.01 mm). Measurements at the base, center, and tip of each probe were averaged to determine the L_{PHY} for each of the 12 sensors. Effective probe spacing was determined by using a calibration procedure (Kluitenberg, 2002) that involved making measurements in water immobilized with 4 g L^{-1} agar. This procedure resulted in two unique L_{EFF} values for each sensor, one obtained using the ILS model and one obtained using the ICPC model.

Two experiments were conducted to evaluate the sensor performance in porous media. In Exp. I, all four sensor types (Table 2) were used to measure the volumetric water content of air-dry and saturated glass beads and Tottori sand. The results

from this experiment were used to identify the R-DPHP sensor design with the optimal probe length. In Exp. II, measurements were conducted using only the R-DPDP sensor identified as having probes of optimal length. All four porous media were used in this experiment, and measurements were performed within four ranges of volumetric water content: 0 to 4 (air dry), 10 to 15, 20 to 25, and 36 to 43% (saturated). Within each of these ranges, the water content varied among the porous media because of differences in bulk density and texture.

In both experiments, the porous media were packed into brass cylinders (8-cm diameter, 6-cm height). Using one sensor per cylinder, inserted through a slot in the cylinder wall, the probes were placed horizontally midway along the height of each core (Fig. 1). A dry-packing procedure was used to prepare the samples of glass beads and Tottori sand that were used for the air-dry and saturated measurements. After installing the sensor and filling the entire cylinder with air-dry material, the top rim of the cylinder was tapped repeatedly until the desired bulk density was achieved. Following completion of the air-dry measurements, the samples were saturated by adding de-aired water from the bottom through filter paper that had been fixed to the bottom of the cylinders. The samples were covered to minimize evaporation before and during heat-pulse measurements.

Intermediate water contents for the glass beads and Tottori sand and water content from dry to saturation for the Columbia and Yolo soils were obtained by mixing predetermined amounts of dry material with water. Moist soil was added to the brass cylinders in layers that were approximately 1 cm in height. After packing each layer with a plunger, the soil surface was roughened to minimize layering effects. These soil cores were closed with airtight plastic covers to minimize water content changes by either drainage or evaporation before and during the measurements.

The experiments were conducted in a controlled-temperature room at 20 $\pm$ 1°C. Heat-pulse measurements were initiated at least 12 h after completion of the soil packing to allow for both hydraulic and thermal equilibrium. The intermediate water contents of all media were small enough that water redistribution due to gravity was minimal. The actual water content and bulk density of all samples were gravimetrically determined by weighing them before the experiments and again after oven drying. Bulk density varied between 1350 and 1650 kg m^{-3}, depending on the degree of saturation and medium type. These bulk density values were used to determine the volumetric water content with the DPHP method.

Table 4. Properties of the porous media used in this study.

Material	Characteristics†	Specific heat‡
		J kg^{-1} K^{-1}
Glass beads	0.5-mm mean diameter (0.4–0.6-mm-diameter range)	738
Tottori sand	0.28-mm mean diameter (95% with 0.149–0.5-mm-diameter range) (Toride et al., 2003)	735
Columbia sandy loam	63.2% sand, 27.5% silt, 9.3% clay (Chen et al., 1999)	800
Yolo silt loam	23.0% sand, 55.5% silt, 22.5% clay (Eching et al., 1994)	817

† Particle size was not evaluated in this study; values and references are provided for the general characteristic of the soil.

‡ Mean of three replicates, determined at 23°C by Thermophysical Properties Research Laboratory, West Lafayette, IN.

Resistance to Probe Deflection

Because the ILS and ICPC models are both two dimensional, they assume that the probes are infinitely long. Thus, the probes must be long enough to satisfy that assumption. However, longer probes are more likely to deflect during sensor installation. Therefore, we analyzed probe deflection as a function of the diameter, wall thickness, and length of the stainless steel tubing. This was done by using solutions of the Euler–Bernoulli equation for cantilever beam deflection (Beer et al., 2006). Specifically, we used two solutions that correspond to two different distributions of force along the beam. For the first case (Fig. 2a), we assumed that a force F is applied at the tip of the probe, mimicking the situation where a local obstacle is encountered during insertion of the probes into the soil. The second case (Fig. 2b) considered a homogeneous load P (force per unit length) applied along the entire length of the probe length, mimicking the situation where the entire probe is under stress. The solutions of the Euler–Bernoulli equation for these two cases are (Beer et al., 2006)

$$\delta_1 = \frac{Fl^3}{3EI} \quad [1a]$$

$$\delta_2 = \frac{Pl^4}{8EI} \quad [1b]$$

where l is beam length and δ is beam deflection. The material properties that characterize the mechanical behavior of the beam are Young's modulus of elasticity, E, and the second moment of area, I. The second moment of area for tubing can be calculated by (Beer et al., 2006)

$$I = \frac{\pi \left(od^4 - id^4 \right)}{64} \quad [2]$$

We used Eq. [1] to determine the relative differences in deflection among the probes. This makes it unnecessary to specify values for the constants F, P, and E. To make relative comparisons, i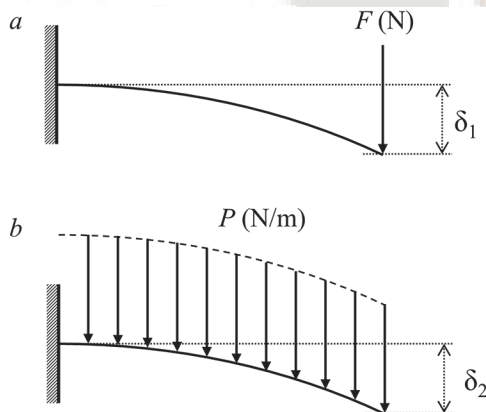t is necessary only to assume that the probes being compared are subject to the same load and are made from the same material. Using δ_R for the deflection of a reference probe and δ for the deflection of any other probe of interest, we introduce a relative resistance-to-deflection parameter σ (dimensionless), defined as

$$\sigma = \frac{\delta_R}{\delta} \quad [3]$$

Substituting Eq. [1] and [2] into Eq. [3] yields the expressions

$$\sigma_1 = \frac{l_R^3}{od_R^4 - id_R^4} \cdot \frac{od^4 - id^4}{l^3} \quad [4a]$$

$$\sigma_2 = \frac{l_R^4}{od_R^4 - id_R^4} \cdot \frac{od^4 - id^4}{l^4} = \sigma_1 \frac{l_R}{l} \quad [4b]$$

where od is the outer dimension of the probe, id is the inner dimension of the probe, and the subscript R denotes the dimensions of the reference probe. Values for σ_1 and σ_2 were obtained by using the probes of the C-DPHP sensor as the reference (Table 2, i.e., $id_R = 0.838$ mm, $od_R = 1.27$ mm, and $l_R = 28$ mm). We note that the contribution of the epoxy filling to deflection was neglected in this analysis.

Heat Conduction Models

Consider a DPHP sensor with infinitely long probes that have a radius a_0 and volumetric heat capacity C_0. The probes, with centerlines a distance L apart, are surrounded by soil with a bulk volumetric heat capacity C, bulk thermal conductivity λ, and bulk thermal diffusivity κ, where $\kappa = \lambda/C$. It is assumed that the soil is homogeneous and isotropic, that its thermal properties are temperature independent, and that it is in perfect thermal contact with the probes. We use $T(t)$ for the temperature of the temperature probe, where t is time. Heat is released at rate per unit length q' during the finite time interval $0 < t \le t_0$, where t_0 is the heating duration.

For the limiting case where the radius of the probes is infinitely small (i.e., $a_0 \to 0$), $T(t)$ becomes equivalent to the temperature of the soil at distance L from a line heat source. The solution of the heat conduction equation for this limiting case is the ILS solution (Bristow et al., 1994a; de Vries and Peck, 1958):

$$T(t) = \begin{cases} -\dfrac{q'}{4\pi\lambda}\,\mathrm{Ei}\!\left(\dfrac{-L^2}{4\kappa t}\right); & 0 < t \le t_0 \\[2ex] \dfrac{q'}{4\pi\lambda}\left\{\mathrm{Ei}\!\left[\dfrac{-L^2}{4\kappa(t-t_0)}\right] - \mathrm{Ei}\!\left(\dfrac{-L^2}{4\kappa t}\right)\right\}; & t > t_0 \end{cases} \quad [5]$$

where $-\mathrm{Ei}(-x)$ is the exponential integral of argument x. This solution is appropriate for use if the ratio a_0/L is sufficiently small or if the thermal properties of the probes do not differ substantially from those of the soil.

Fig. 2. Illustration of (a) force, *F*, and (b) load, *P*, scenarios considered for calculating deflection using the Euler–Bernoulli equation for cantilever beam deflection (after Beer et al., 2006).

Although an analytical solution is not available for the case where the probes have finite radius and finite thermal properties, Knight et al. (2012) presented an approximate solution that accounts for the finite radius and finite heat capacity of the probes. They derived their solution by considering the probes to be infinitely long cylindrical perfect conductors, making the simplifying assumption that the probes have infinite thermal conductivity. The ICPC solution, which is a special case of their general solution, considers that the heater and temperature probes both have the same radius and the same volumetric heat capacity.

The ICPC model begins with the Laplace-domain solution, which represents the case where heat is released continuously at rate q', given as (Knight et al., 2012)

$$\hat{T}_C(p)=$$

$$\frac{q'K_0(\mu L)}{2\pi\lambda p\left\{\mu a_0\left[K_1(\mu a_0)+(\mu a_0\beta_0/2)K_0(\mu a_0)\right]\right\}^2} \quad [6]$$

in which p is the Laplace transform parameter and $\hat{T}_C(p)$ represents the Laplace transform of $T_C(t)$, which is the temperature of the temperature probe for the case of continuous heating. In this expression, $\mu=\sqrt{(p/\kappa)}$, $\beta_0=C_0/C$, and $K_n(z)$ denotes the modified Bessel function of the second kind of order n and argument z. The Laplace domain solution, Eq. [6], is numerically inverted for two cases: $T_C(t)$ and $T_C(t-t_0)$ (Knight et al., 2012; Stehfest, 1970a, 1970b). To obtain $T(t)$, the temperature of the temperature probe for the case where the duration of heating is finite, the principle of superposition in time is applied. This is implemented by substituting $T_C(t)$ and $T_C(t-t_0)$ into

$$T(t)=\begin{cases} T_C(t); & 0<t\leq t_0 \\ T_C(t)-T_C(t-t_0); & t>t_0 \end{cases} \quad [7]$$

Equations [6] and [7], which together represent the ICPC solution, are identical to Eq. [40a] and [40b], respectively, of Knight et al. (2012).

To implement the ICPC solution, the radius and volumetric heat capacity of the probes must be known. The outer radius of the probes, a_0, is either known from the manufacturer (as in our case, the outer diameter of the stainless steel tubing, Table 2) or can be easily measured. However, the determination of C_0 must take into account the fact that the probes are composite solids. In this study, the probes were made from stainless steel tubing and thermally conductive epoxy having volumetric heat capacities of $C_{SS}=4.00$ MJ m^{-3} K^{-1} and $C_E=2.03$ MJ m^{-3} K^{-1}, respectively. The value used for C_{SS} is from data of the European Stainless Steel Development Association for Type 316 stainless steel at 20°C, whereas the value of C_E is the mean of three replicate samples, determined at 23°C by the Thermophysical Properties Research Laboratory. The value of C_0 is the volume average of the heat capacities of these two materials, calculated as

$$C_0=C_E\frac{a_E^2}{a_0^2}+C_{SS}\left(1-\frac{a_E^2}{a_0^2}\right) \quad [8]$$

where a_E is the radius of the epoxy-filled region, equal here to the inner radius of the stainless steel tubing (taken from inner diameter values in Table 1, as given by the manufacturer). Using Eq. [8] with the heat capacity values above and the dimensions from Table 1, the resulting C_0 values are 3.14 and 3.68 MJ m^{-3} K^{-1} for the C-DPHP and the R-DPHP sensors, respectively. The probe heat capacity is greater for the R-DPHP sensor because its probes contain a greater proportion of stainless steel. For the case of measurements in water ($C=4.18$ MJ m^{-3} K^{-1}), the β_0 values are 0.75 and 0.88 for the C-DPHP and R-DPHP sensors, respectively, indicating that C_0 for the R-DPHP sensor is much closer to the volumetric heat capacity of water. This is important when calibrating L_{EFF} from measurements in immobilized water.

Parameter Estimation and Data Analysis Procedures

Thermal properties were estimated from DPHP temperature measurements by minimizing the objective function (OF):

$$\text{OF}=\sum_{i=1}^{n}\left[T_S(t_i)-T_M(t_i,\mathbf{p})\right]^2 \quad [9]$$

where $T_S(t_i)$ is the temperature of the DPHP sensor at time t_i, $T_M(t_i,\mathbf{p})$ is the temperature from either the ILS or the ICPC model, and $\mathbf{p}$ is a vector of optimized parameters. The sensor temperature data used to minimize the objective function were taken from a 5-s time interval centered on the time at which the maximum temperature rise occurred. Because sensor data were collected with a measurement frequency of 120 Hz, the optimization was conducted using $n=11$. This approach is a hybrid of the single-point method (e.g., Ren et al., 1999) and the method that involves fitting of the entire temperature response curve via optimization (e.g., Hopmans et al., 2002). Whereas the single-point method is sensitive to measurement errors of a single data point, fitting of the entire curve minimizes the impact of measurement errors (Bristow et al., 1995). Compared with data from early times, data from later times are more sensitive to spatial regions farther away from the probes (Kluitenberg et al., 1993). This means that data from later times are influenced to a greater extent by the finite length of the probes and the body of the sensor, which are not taken into account in the models. Additionally, data from times near the temperature maximum have the greatest measurement/noise ratio. For these reasons, we believe that the hybrid approach minimizes bias in the estimated thermal properties that can be introduced when using either a single point or the entire temperature response curve. We revisit this issue below in our discussion of the experimental results.

When optimizing for the effective probe spacing, L_{EFP} in the calibration process, we used the parameter vector $\mathbf{p}=(L_{EFP},\lambda)$, and the volumetric heat capacity was fixed to that of water ($C_W=4.18\times10^6$ J m^{-3} K^{-1}). Optimization for soil thermal properties was conducted by using $\mathbf{p}=(C,\lambda)$ and a fixed

value for the probe spacing, either L_{EFF} or L_{PHY}. Subsequently, the optimized C value was used to calculate the volumetric water content, θ (Kluitenberg, 2002):

$$\theta = \frac{C - \rho_b c_s}{C_W} \qquad [10]$$

where c_s ($J\,kg^{-1}\,K^{-1}$) is the specific heat of the solid phase and ρ_b ($kg\,m^{-3}$) denotes the dry soil bulk density.

Values of c_s are needed for evaluating θ with Eq. [10]. In this study, θ was evaluated using the c_s values determined by differential scanning calorimetry. However, when θ is known (such as by gravimetric measurements), independent c_s values can be obtained by rearranging Eq. [10] to give

$$c_s = \frac{C - \theta C_W}{\rho_b} \qquad [11]$$

Like Eq. [10], this expression is evaluated using DPHP-estimated C and gravimetrically measured ρ_b values (Campbell et al., 1991).

RESULTS AND DISCUSSION
Probe Deflection Analysis

The expressions for σ_1 and σ_2 in Eq. [4] were used to examine how probe rigidity is influenced by the dimensions of the stainless steel tubing, namely the inner diameter, outer diameter, and length. In Fig. 3, values of σ_1 and σ_2 are presented as functions of the probe length for both the C-DPHP and R-DPHP sensors. The symbols on the curves correspond to the four sensors in Table 2. Recall that the parameters σ_1 and σ_2 quantify deflection resistance relative to the deflection resistance of the probes of the C-DPHP sensor. Thus, resistance to deflection is equivalent to that for the conventional sensor when $\sigma_1 = 1$ or $\sigma_2 = 1$.

As expected, for all probes, the resistance to deflection decreased as the probe length increased (Fig. 3). However, the deflection potential was much less for the larger diameter probes because of increased wall thickness. Consequently, although resistance to deflection decreased with probe length, its value for the longest of the large-diameter probes was still greater than that for the conventional probe. Assuming that the two force distributions in Fig. 2 represent limiting cases of various force distribution possibilities, it follows that, in reality, the probes are exposed to a force distribution lying somewhere between these two limiting cases. Consequently, the actual resistance to deflection lies somewhere between σ_1 and σ_2. The results show that, relative to the C-DPHP sensor, the gain in resistance to deflection is between 6.1 and 7.6 for the R-DPHP-35 sensor, between 3.6 and 5.1 for the R-DPHP-40 sensor, and between 2.2 and 3.6 for the R-DPHP-45 sensor. We refer to these results below when we discuss the need to compromise between the enhanced rigidity achieved with shorter probes and the gain in accuracy achieved when soil properties are determined with longer probes.
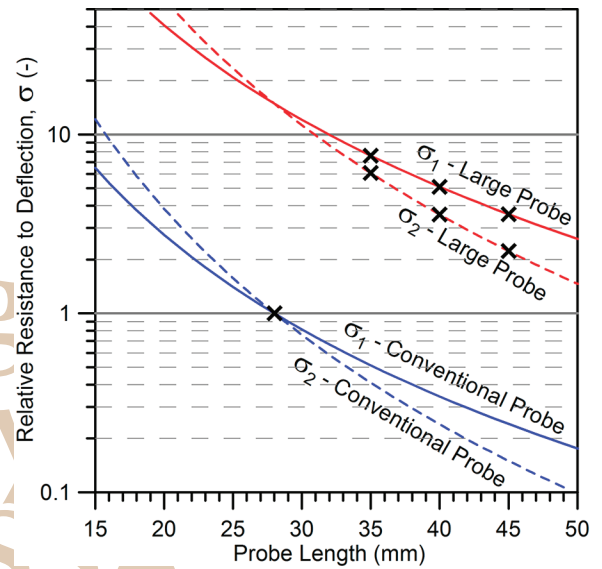

Fig. 3. Relative resistance to deflection (σ) for the force and load scenarios, σ_1 and σ_2, respectively. The markers on the curves correspond to the four sensors that were tested.

Sensor Calibration

Calibration results for all 12 sensors (three replicates of each of the four sensor types) are presented in Table 5 for both the ILS and ICPC models. These results include optimized values of the effective probe spacing (L_{EFF}) and thermal conductivity. For comparison, values of the physical probe spacing (L_{PHY}) are also included in Table 5. Optimized values of conductivity were compared with the conductivity of water at 20°C, which is 0.595 W m^{-1} K^{-1}. Although the L_{EFF} values determined with both models were in good agreement with the physical spacing, with differences not larger than about 2%, estimates of thermal conductivity obtained with the ILS model deviated significantly from the expected value of 0.595 W m^{-1} K^{-1}, with errors as large as 9%, suggesting significant bias in the ILS model.

The bias in λ estimates obtained with the ILS model (Table 5) is due in part to the fact that the heat capacity of the probes differs from that of water, but this has only minimal effect because the difference in heat capacity is relatively small, especially for the R-DPHP sensors. The primary reason for bias in these λ estimates is related to the fact that the thermal conductivity of the probes is much greater than that of water. Because the ILS model does not account for this, it yields conductivity estimates that are not representative of the immobilized water alone. Instead, it yields conductivity estimates representative of the composite media–probe system, which results in overestimation of the water's thermal conductivity. In contrast to the results obtained with the ILS model, conductivity estimates obtained with the ICPC model revealed only minimal error and no consistent bias (Table 5). To some extent, this is due to the fact that the ICPC model accounts for the finite heat capacity of the probes; however, for the case considered here (i.e., measurements in water), the ICPC model yielded better λ estimates primarily because it accounted for the fact that the probes and water have different conductivities. Indeed, the ICPC model assumes that the probes are perfect

Table 5. Effective probe spacing (L_{EFF}) and thermal conductivity (λ) of the conventional (C-DPHP) and rigid dual-probe heat-sensors (R-DPHP) with 35-, 40-, and 45-mm-long probes determined with the infinite line source (ILS) and identical cylindrical perfect conductors (ICPC) models from measurements in immobilized water. Values are given for three replicates (one line per replicate) of each sensor type. Errors in L_{EFF} are relative to physical probe spacing (L_{PHY}). Errors in λ are relative to the conductivity of water at 20°C (0.595 W m^{-1} K^{-1}).

Sensor	L_{PHY}†	Effective probe spacing				Estimated λ			
		ILS		ICPC		ILS		ICPC	
		L_{EFF}	Error	L_{EFF}	Error	λ	Error	λ	Error
	mm	mm	%	mm	%	W m^{-1} K^{-1}	%	W m^{-1} K^{-1}	%
C-DPHP	6.047	6.088	0.68	6.120	1.22	0.623	4.66	0.598	0.54
	6.100	6.131	0.50	6.163	1.04	0.622	4.54	0.597	0.38
	6.043	6.096	0.86	6.128	1.40	0.629	5.72	0.604	1.54
R-DPHP-35	7.149	6.988	−2.24	7.043	−1.48	0.642	7.89	0.592	−0.51
	7.139	7.105	−0.47	7.159	0.28	0.650	9.27	0.601	1.07
	7.145	6.987	−2.22	7.041	−1.46	0.649	9.09	0.600	0.78
R-DPHP-40	7.085	6.938	−2.08	6.993	−1.30	0.648	8.96	0.598	0.47
	7.142	7.022	−1.69	7.076	−0.93	0.651	9.45	0.602	1.13
	7.152	7.053	−1.38	7.107	−0.63	0.640	7.54	0.592	−0.48
R-DPHP-45	7.099	6.940	−2.24	6.995	−1.47	0.648	8.92	0.598	0.45
	7.162	7.075	−1.22	7.129	−0.47	0.649	9.06	0.599	0.74
	7.172	7.123	−0.69	7.176	0.06	0.650	9.21	0.602	1.11

† Average of three caliper measurements taken at the base, center, and tip of the probes.

conductors, but this assumption turns out to be quite reasonable because the thermal conductivity of the probes is substantially greater than that of water.

As part of this study, we explored the possibility of omitting the calibration procedure by using the physical probe spacing, L_{PHY}, instead of L_{EFF}. Although L represents the distance between the heater and temperature probes in both the ILS model (Eq. [5]) and ICPC model (Eq. [6] and [7]), its physical meaning in these models is slightly different. Whereas the ILS solution neglects the properties of both probes, the ICPC solution accounts for their finite radius and heat capacity. Therefore, when the two models are fitted to temperature data from the same sensor, the fitted L values (denoted by the effective probe spacing, L_{EFF}) will probably be different. Although L_{EFF} will differ from the true physical probe spacing (L_{PHY}) in both models, their values must be close if either model provides a good approximation to heat transport of the sensor–medium system. It is interesting, however, that a clear model effect is not evident in the error of the L_{EFF} estimates (Table 5). The ICPC model produced smaller errors in L_{EFF} estimates for the R-DPHP sensors, whereas the ILS model produced smaller errors in L_{EFF} estimates for the C-DPHP sensors. This is of interest because one would naturally expect the more physically correct ICPC model to consistently yield L_{EFF} values closer to the physical probe spacing. This inconsistency probably has to do with the fact that both models contain factors of $L/\sqrt{(\kappa)}$. Thus, to some extent, neither model allows entirely unique estimates of probe spacing and conductivity, and it appears that agreement between L_{EFF} and L_{PHY} is, by itself, an insufficient indicator of model performance. However, when considered together with the results for thermal conductivity determination, it certainly appears that the ICPC model provides considerable improvement over the ILS model, at least for the sensor types considered here.

Experiment I

In this experiment, all 12 sensors (three replicates of each of the four sensor types) were used to measure the volumetric water content of glass beads and Tottori sand for both air-dry and saturated conditions. Water content was determined using both the ILS and ICPC models, but with effective probe spacing only. The results (Fig. 4) are expressed as the deviation in volumetric water content ($\Delta\theta$) between DPHP-measured water contents and those determined gravimetrically by oven drying and mass balance, with the latter assumed to be the known or actual water contents. The results for air-dry conditions (Fig. 4a and 4b) show a similar deviation in water content for both glass beads and Tottori sand. We note that the error for results obtained with the C-DPHP sensor in dry media is smaller than that of the R-DPHP sensor, especially with the ILS model. The overestimation of water content with the C-DPHP sensor and the ILS model is consistent with findings in previous studies (Basinger et al., 2003; Bristow et al., 2001; Heitman et al., 2003; Ren et al., 2003). With the exception of one measurement, for all of the R-DPHP sensors, both heat conduction models resulted in overestimation of the water content ($\Delta\theta > 0$), with deviations decreasing as the probe length increased. However, water content overestimation was much greater for the ILS model (Fig. 4a), with a maximum error of about 0.09 m^3 m^{-3} for the shortest probe (R-DPHP-35). Owing to their larger diameter and relatively large heat capacity, the probes of the R-DPHP sensors caused a reduction in the maximum temperature rise, which caused the ILS model to overestimate the heat capacity, thereby resulting in overestimation of the water content. We therefore conclude that, in air-dry media, water content results for the R-DPHP sensors are unacceptable with the ILS model.

In contrast to the relatively poor performance of the ILS model, the ICPC model showed very good results under dry
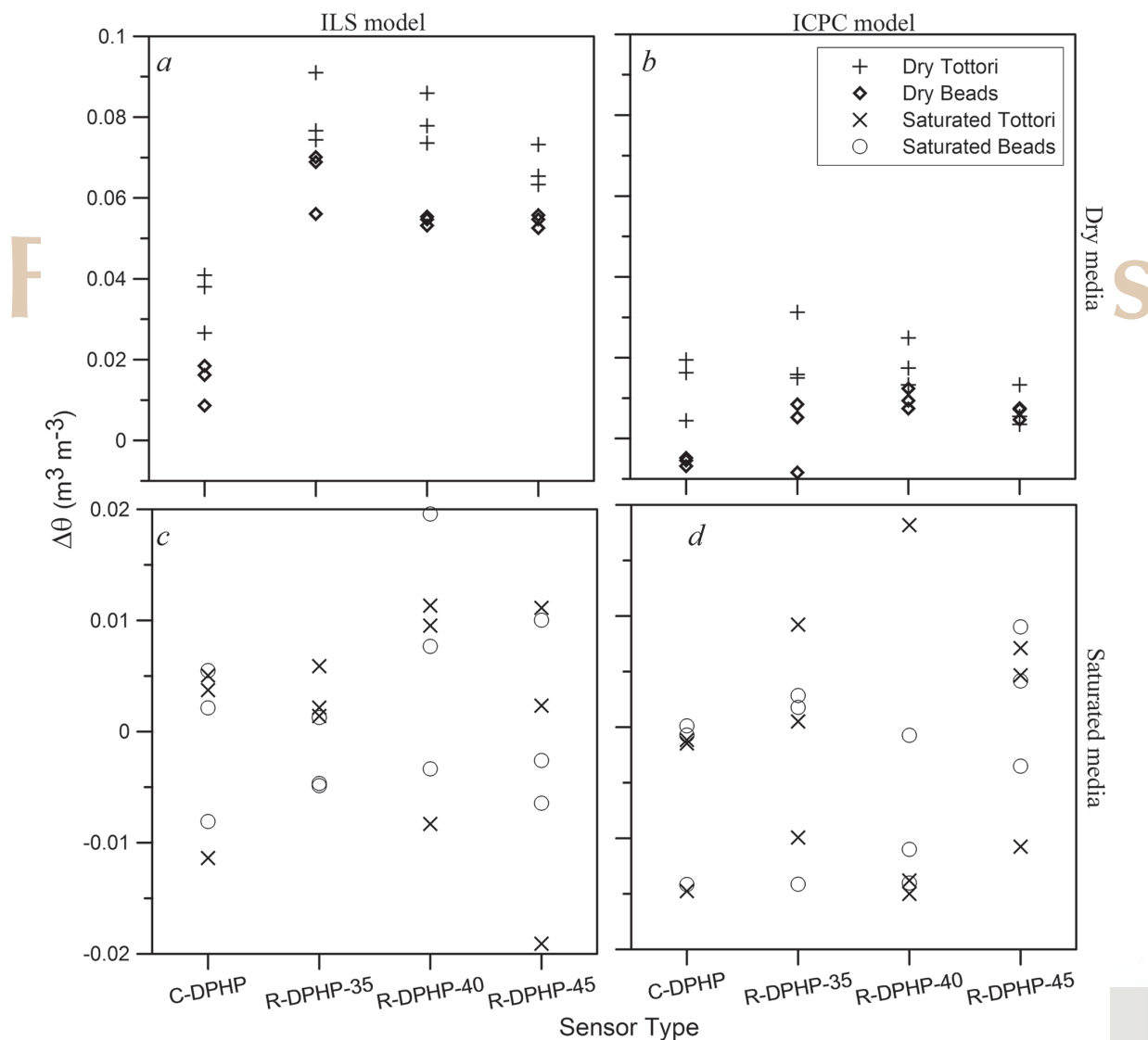
Fig. 4. Difference in volumetric water content ($\Delta\theta$) between water content results from the dual-probe heat-pulse (DPHP) method and those obtained gravimetrically. Results are shown for two media (glass beads and Tottori sand), two soil water content levels (dry and saturated), and four sensor types (conventional DPHP [C-DPHP], DPHP with 35-mm-long rigid probes [R-DPHP-35], DPHP with 40-mm rigid probes [R-DPHP-40], and DPHP with 45-mm rigid probes [R-DPHP-45]), with three replicates each. For each sensor type, results obtained with both the infinite line source (ILS) model and the identical cylindrical perfect conductors (ICPC) model are shown.

conditions, with overestimation of the volumetric water content not exceeding 0.035 m³ m⁻³ but mostly smaller and decreasing with increasing probe length. The finite length of the probes and the presence of the sensor body are possible reasons for these deviations from the ICPC model because the model assumes that the probes are infinite in length. In both the heater and temperature probes, energy is lost because of their finite length. In the heater probe, heat is lost to the surrounding porous medium and the sensor body in the axial direction; in the temperature probe, the energy beyond the tips of the probe in the axial direction is not entirely captured. These energy losses cause a lower temperature response at the temperature probe, thereby resulting in overestimation of the soil's heat capacity and its corresponding volumetric water content.

Results from the measurements in saturated media (Fig. 4c and 4d) show excellent performance by both the ILS and ICPC models, with deviations in volumetric water content not larger than about 0.01 m³ m⁻³ in most cases and minimal influence of sensor type. In saturated media, the probes and the medium surrounding them have nearly the same volumetric heat capacity. Thus, the fact that the ICPC model accounts for the finite heat capacity of the probes does not improve on the accuracy in water content estimation achieved with the ILS model. Our results under saturated conditions also show that, for both models, accuracy is not affected by the finite length of the probes. This is explained by the high thermal conductivity of the saturated porous media, causing early arrival of the heat pulse maximum and thereby minimizing the thermal losses mentioned above.

Experiment II

Based on results of the resistance-to-deflection analysis and Exp. I, further evaluation was conducted using only the

R-DPHP-40 sensor in combination with the ICPC model. The probes of this sensor are about four to five times more rigid than those of the C-DPHP sensor (Fig. 3), and its measurement performance is nearly equivalent to that of the R-DPHP-45, which produced the most accurate water content estimates (Fig. 4). For further evaluation of the R-DPHP-40 sensor, the three replicate sensors of this type were tested in all four porous media within four ranges of water content. Water content estimates were obtained with the ICPC model by using the calibrated effective probe spacing (Fig. 5, left column) as well as the measured physical spacing (Fig. 5, right column). The first important observation that can be determined from Fig. 5 is that there is generally no evidence of soil-specific effects on the soil water content measurements, including the variation among replicates. Second, we observe that use of the ICPC model with L_{PHY} resulted in slightly larger variations among replicates than their equivalents using L_{EFF}, especially at or near saturation. Because the thermal conductivity of saturated media is relatively high, errors in measurement of the physical probe spacing could be the source of these variations.

To quantify the performance of the R-DPHP-40 sensor, we grouped the results for all four media together (Fig. 6) for linear regression analysis and determination of the root mean square error (RMSE). The slope and intercept of a linear regression model provide quantification of systematic bias from the 1:1 line, whereas RMSE quantifies deviation from the 1:1 line and provides a measure of sensor precision. The results (Fig. 6) indicate that the precision of the R-DPHP-40 sensor is excellent, with RMSE volumetric water content values of 0.014 and 0.021 m^3 m^{-3} using effective and physical probe spacing, respectively. Inferences regarding the slopes and intercepts of the two regression models (Fig. 6) were made by calculating the 95% confidence intervals for those regression parameters. For both models, we concluded that the slope and intercept were not significantly different from unity and zero, respectively. Thus, for both of the approaches used to quantify probe spacing
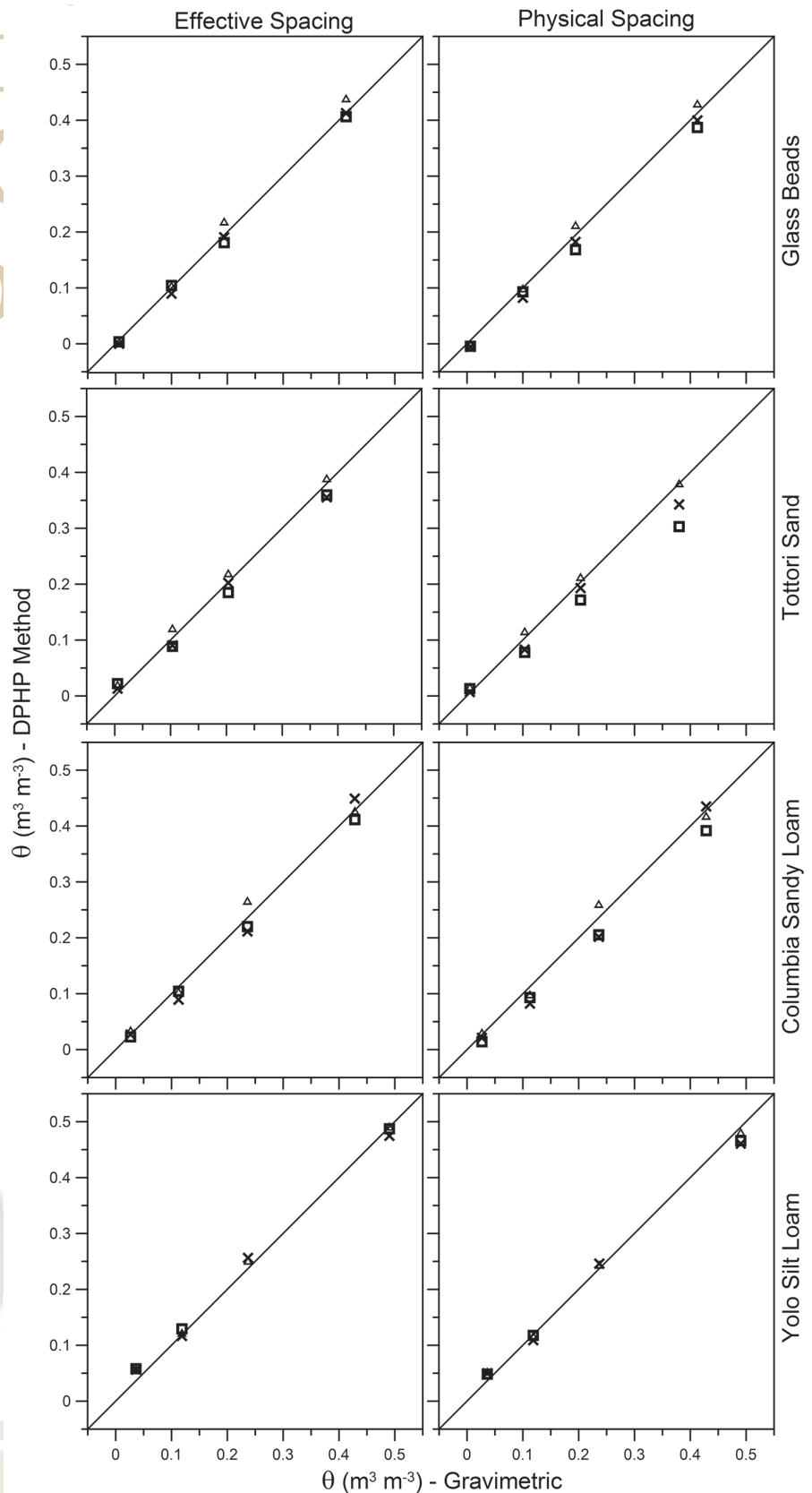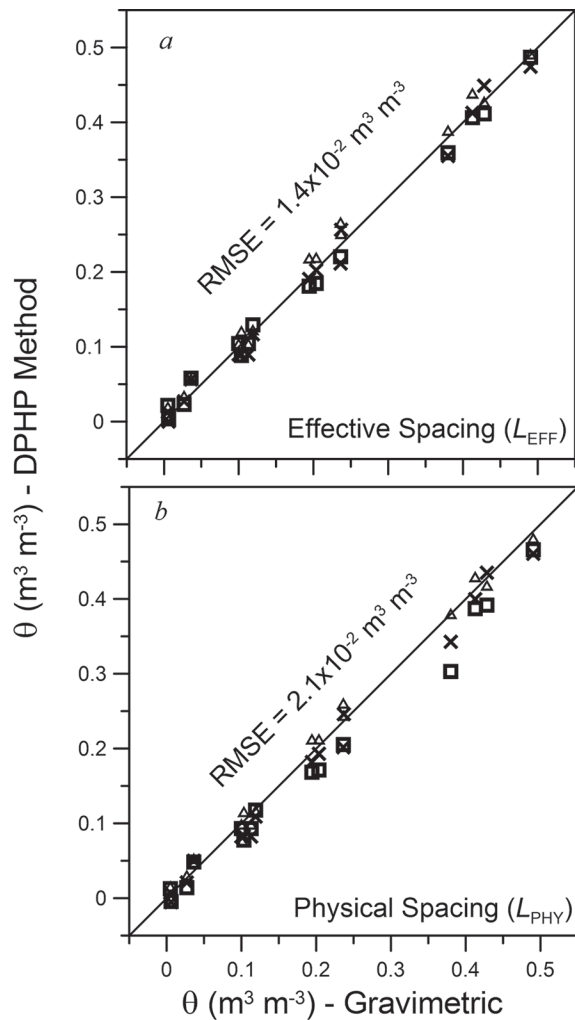

Fig. 5. Comparison of volumetric water content (θ) as determined by rigid dual-probe heat-pulse (R-DPHP) and gravimetric methods for the four porous media. The DPHP measurements were obtained with the R-DPHP-40 sensor (probes 2.38 mm in diameter and 40 mm long) in conjunction with the identical cylindrical perfect conductors (ICPC) model. Water content results from the DPHP method were obtained using both calibrated effective probe spacing (left panels) and physically measured probe spacing (right panels). The different symbols represent values from the three replicate sensors.

Fig. 6. Comparison of volumetric water content (θ) as determined by rigid dual-probe heat-pulse (R-DPHP) and gravimetric methods for all four porous media combined. The DPHP measurements were obtained with the R-DPHP-40 sensor (probes 2.38 mm in diameter and 40 mm long) in conjunction with the identical cylindrical perfect conductors (ICPC) model. Water content results from the DPHP method were obtained using both (a) calibrated effective probe spacing and (b) physically measured probe spacing. The different symbols represent values from the three replicate sensors; RMSE values are given with reference to the 1:1 line. Linear regression shows $y = 0.984x + 0.003$ with $r^2 = 0.992$ for the top plot and $y = 0.987x + 0.002$ with $r^2 = 0.987$ for the bottom plot.

(i.e., effective and physical), water content estimates obtained with the R-DPHP-40 sensor were found to be unbiased. To determine if the sensor is soil independent (i.e., if pooling of the data is justified), linear regression analysis was conducted to calculate slopes and intercepts for the eight individual data sets in Fig. 5. Slopes and intercepts for the data in the left column of Fig. 5 were found to lie within the respective 95% confidence intervals for the slope and intercept of the regression model in Fig. 6a. Testing of the results from the right column of Fig. 5 yielded the same outcome. Thus, we conclude that the proposed sensor, when used in conjunction with the ICPC model, measures soil water content without systematic bias and is soil independent.

Although excellent results were obtained by using the ICPC solution together with large-diameter probes, we note

that measurement errors in volumetric water content using gravimetric methods are typically on the order of 1% (v/v) or larger. Additional uncertainty arises from the fact that the sampling volume of a DPHP sensor is small relative to the volume of the sample used to independently determine water content via oven drying. Hence, for any comparison with gravimetric water content data, we must accept deviations between 1 and 2% (v/v) at a minimum. Considering this magnitude of error, we should not expect the results of sensor measurements better than our comparison in Fig. 6, which resulted in RMSE values between 0.014 and 0.021 m³ m⁻³.

The specific heat of the solid phase, c_s, was independently measured via differential scanning calorimetry, and those values were used for determining θ with Eq. [10]. However, as Campbell et al. (1991) originally suggested, values of c_s can be obtained directly from DPHP measurements by using Eq. [11] with DPHP-estimated C values and gravimetrically evaluated θ and ρ_b values. Table 6 summarizes the results of c_s values obtained in this way with the R-DPHP-40 sensor and the ICPC model, determined under air-dry conditions for the four porous media. Apart from the results for Yolo silt loam, errors in c_s estimates are within 5% (Table 6). Most previous studies do not have independent c_s measurements to compare with DPHP-estimated c_s values (e.g., Tarara and Ham, 1997; Ren et al., 2003) but rather rely on either c_s calculations using the mixing model of mineral and organic matter (Kluitenberg, 2002) or previously published values. Most of these studies recognized significant overestimation of c_s with the DPHP method using the C-DPHP sensor and the ILS model. Furthermore, Ren et al. (2003) used their DPHP-estimated c_s values to correct for bias in DPHP-estimated θ, although these c_s values were much higher (>10%) than literature values. In this study, however, we postulated that the R-DPHP-40 sensor and the ICPC model do not yield systematic errors in c_s values, as already seen for θ estimation. Thus, we recommend the proposed method for measuring specific heat.

Additional Insights

The ICPC model, combined with the large-diameter and longer probes, presents a major advantage over the combination of ILS theory and conventional DPHP probes. Not only does the ICPC model account for the disparities observed using the ILS model, it captures the major heat transfer processes. This is so, despite the fact that it (i) only partially accounts for the finite conductivity of the probes; (ii) averages the heat capacity of the probe materials (thermally conductive epoxy and stainless steel) and ignores the heater wire and thermistor; (iii) neglects the finite length of the probes; (iv) does not incorporate the properties of the sensor body; and (v) assumes perfect thermal contact between the probes and the surrounding porous media. Yet, with all these simplifications, the results of our regression analysis suggest that the estimation of θ is very accurate across a wide range of water contents and is independent of soil type.

It is no coincidence that the ICPC model performed well with the presented DPHP sensors because these were

Table 6. Specific heat (c_s) of the porous media as determined by differential scanning calorimetry (DSC) and by evaluating Eq. [11] with results from Exp. II, using the rigid dual-probe heat-pulse method with 40-mm probe length (R-DPHP-40). Measurements with the R-DPHP-40 in air-dry media were used to calculate c_s using both effective probe spacing (L_{EFF}) and physical probe spacing (L_{PHY}). Errors are relative to the DSC-derived c_s results.

Material	DSC c_s†	R-DPHP-40			
		L_{EFF}		L_{PHY}	
		c_s	Error	c_s	Error
	—— J kg^{-1} K^{-1} ——		%	J kg^{-1} K^{-1}	%
Glass beads	738	726	−1.6	710	−3.8
Tottori sand	735	772	5.1	751	2.1
Columbia sandy loam	800	803	0.4	784	−2.1
Yolo silt loam	817	881	7.8	859	5.1

† Mean value of three replicates, determined at 23°C by Thermophysical Properties Research Laboratory, West Lafayette, IN.

constructed to satisfy the assumptions inherent in the ICPC model. Specifically, the thick-walled stainless steel probes filled with silver thermally conductive epoxy were chosen to satisfy the assumption that the probes have infinite thermal conductivity. Moreover, to satisfy the assumption of infinite probe length, despite being larger in diameter, we designed and tested longer probes. Thus, although there remains room for improvement in sensor design and construction, the simplicity of the analytical ICPC model is very attractive for practical soil water content measurement applications. In addition, the thicker probes minimize probe deflection, thereby easing concerns during sensor deployment. We note that in applications where deflection is not an issue, the ICPC solution is perfectly suitable when using the conventional DPHP sensor because its use eliminates the typical water content overestimations for dry soil conditions, as predicted by Knight et al. (2012).

The main advantage of using large-diameter probes is the gain in resistance to deflection, but they also offer the advantage of reducing the temperature rise at the interface between the soil and the heater probe. Large-diameter probes have greater surface area, which allows heat energy to be distributed across a larger surface. Consequently, for the same heating rate, the temperature at the probe–soil interface decreases as the diameter of the heater probe increases (Kamai et al., 2008, 2010). Although not analyzed in this study, there are several benefits that may be gained from this lower temperature. A smaller temperature rise at the probe–soil interface may help to avoid processes such as soil water vaporization on soil heating, free water convection due to temperature gradients, and variability in soil thermal properties due to their temperature dependency. It is important that these processes remain insignificant because they are ignored in the ICPC heat conduction model.

Although our study showed significant improvements over existing sensors, we must emphasize that our experiments were done in a laboratory environment, packing soils around the probes, rather than in situ field testing. For field installation of the DPHP sensor, it is likely that the larger diameter probes would require a larger force of insertion, thereby increasing the probability of probe deflection. Moreover, as probe size increases, soil compaction around the probes is likely to be more significant, thereby affecting measurement accuracy. It is for these reasons that we limited the probe diameter to 2.38 mm. However, we note that any sensor insertion into a soil may affect soil density unless insertion holes are drilled before sensor installation, as is commonly done if soil compaction is an issue.

Finally, we examined fits of the ILS and ICPC models to the measured temperature data to discuss fit performance vs. the accuracy of the estimated properties of the heat conduction models. For that purpose, we used typical model–data fit results for immobilized water and for Tottori sand at three different water contents (Fig. 7). First, we note that at relatively late times neither of the two models provided a good fit to the data. This is precisely why we excluded most of the data after the maximum temperature rise in our approach for estimating thermal properties. At relatively late times, the temperature response is influenced by factors not taken into account by the ILS and ICPC models, such as finite probe length, influence of the sensor body, finite sample size, and sample heterogeneity. Second, we draw attention to the fact that, apart from the lack of fit at relatively late times, the degree of fit achieved with the ILS model is as good as that achieved with the ICPC model. This was substantiated by comparing RMSE values that were calculated using measured and modeled temperature data from the first 100 s of each curve in Fig. 7. From this it is evident that the ILS model fit the temperature data well, even though the ILS model yielded biased estimates of water content. Clearly, agreement between the model and the data is, by itself, an insufficient indicator of model performance. Assessment of model performance must also include checks, such as those performed in this investigation, to determine if the DPHP method yields accurate estimates of thermal properties. Additional work is needed to evaluate the accuracy of soil thermal conductivity estimates obtained with the ICPC model and R-DPHP sensor.

CONCLUSIONS

A DPHP sensor with 2.38-mm-diameter probes was evaluated for measuring soil water content. In conjunction with the ICPC solution of Knight et al. (2012), the new sensor was tested under laboratory conditions for a range of soil textures and saturation levels from air dry to fully saturated. The main conclusions of this study include the following:

1. Estimates of volumetric water content obtained with this sensor and model were found to be unbiased compared with independently measured gravimetric water content values.

2. The method is soil independent, provided that the bulk density and specific heat of the solid phase are known. The analysis of pooled data for all porous media showed that soil-specific calibration is unnecessary.

3. Measurement precision is excellent (RMSE = 0.014 m^3 m^{-3}) when probe spacing is treated as an effective parameter (i.e., determined via measurement in immobilized water), but the results obtained using the physical probe spacing (RMSE = 0.021 m^3 m^{-3}) showed minimal loss of precision. Thus, with this sensor and model, it appears that determination of the effective probe spacing is not necessarily required. This, of course, represents a major simplification in the implementation of the DPHP method.

4. Results from a beam-deflection sensitivity analysis showed that, when subject to the same deflection force, the probes of the proposed DPHP sensor are about five times more resistant to deflection than those of conventional DPHP sensors, easing concerns about measurement errors that may stem from probe flexing during installation.

5. The ICPC model improved heat capacity and water content estimation compared with the typically used ILS model, as prior reported overestimation in the dry end was eliminated.

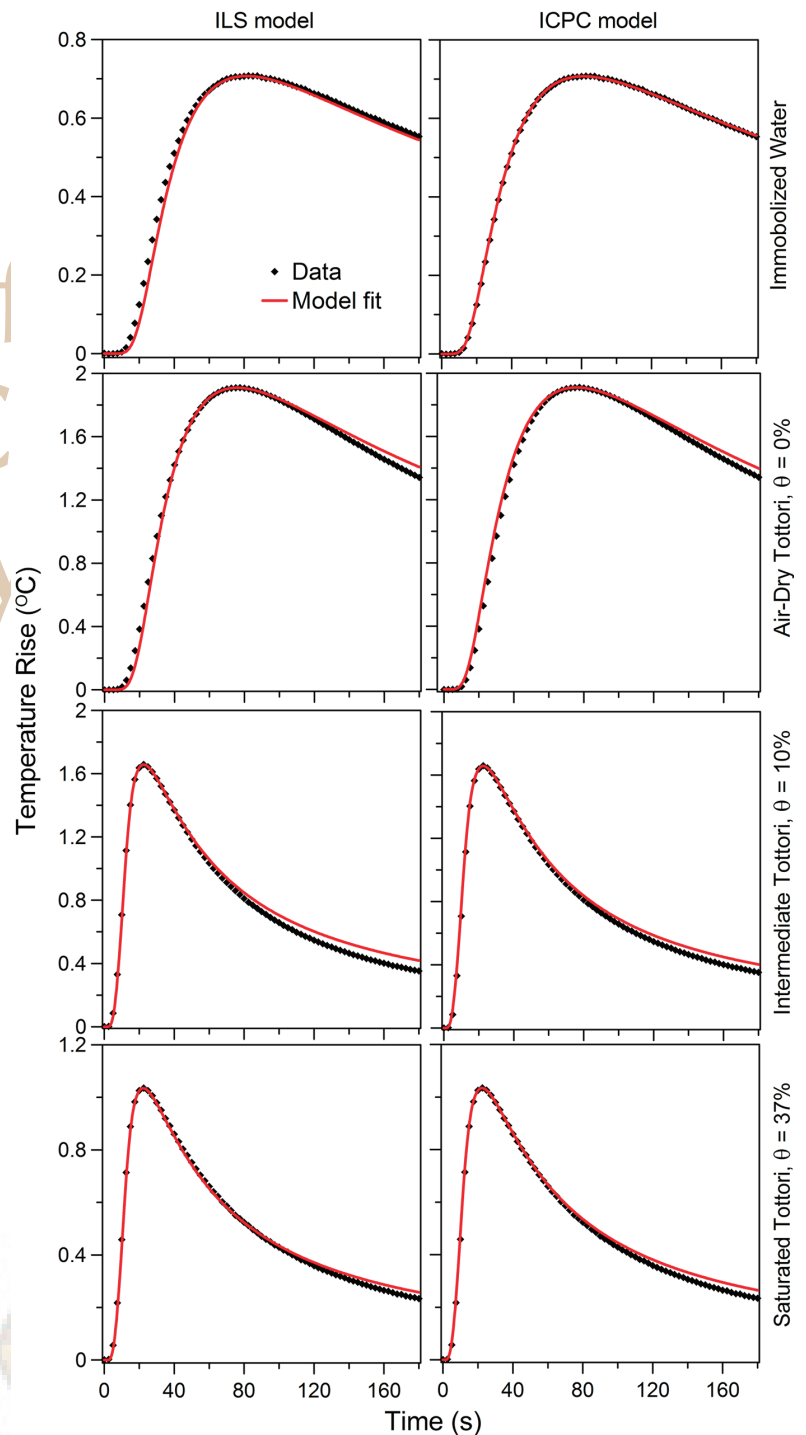6. The method is accurate for measuring c_s, the specific heat of the solid phase.

In summary, we suggest that the presented DPHP sensor, when used in combination with the ICPC heat transport model, provides an excellent alternative to other available water content methods. It is simply based on heat conduction in soils, thereby making the method soil independent. However, a need for further testing and deployment under a wide range of field settings remains. We encourage you to contact us and use this sensor for field deployment and testing.

ACKNOWLEDGMENTS

REFERENCES

Basinger, J.M., G.J. Kluitenberg, J.M. Ham, J.M. Frank, P.L. Barnes, and M.B. Kirkham. 2003. Laboratory evaluation of the dual-probe heat-pulse method for measuring soil water content. Vadose Zone J. 2:389–399. doi:10.2136/vzj2003.3890

Beer, F.P., E.R. Johnston, and J.T. DeWolf. 2006. Mechanics of materials. 4th ed. McGraw-Hill, New York.

Bilskie, J.R., R. Horton, and K.L. Bristow. 1998. Test of a dual-probe, heat-pulse method for determining thermal properties of porous materials. Soil Sci. 163:346–355. doi:10.1097/00010694-199805000-00002

Bristow, K.L. 1998. Measurement of thermal properties and water content of unsaturated sandy soil using dual-probe heat-pulse probes. Agric. For.

Fig. 7. Model fits to temperature response data acquired with the R-DPHP-40 rigid dual-probe heat-pulse sensor (probes 2.38 mm in diameter and 40 mm long). Results are shown for measurements in immobilized water (top) and Tottori sand at different soil water contents (increasing moisture from top to bottom: θ = 0, 10, and 37%) for both the infinite line source (ILS) model (left) and the identical cylindrical perfect conductors (ICPC) model (right).

Meteorol. 89:75–84. doi:10.1016/S0168-1923(97)00065-8

Bristow, K.L., J.R. Bilskie, G.J. Kluitenberg, and R. Horton. 1995. Comparison of techniques for extracting soil thermal properties from dual-probe heat-pulse data. Soil Sci. 160:1–7. doi:10.1097/00010694-199507000-00001

Bristow, K.L., G.S. Campbell, and K. Calissendorff. 1993. Test of a heat-pulse probe for measuring changes in soil-water content. Soil Sci. Soc. Am. J. 57:930–934. doi:10.2136/sssaj1993.03615995005700040008x

Bristow, K.L., G.J. Kluitenberg, C.J. Goding, and T.S. Fitzgerald. 2001. A small multi-needle probe for measuring soil thermal properties, water content and electrical conductivity. Comput. Electron. Agric. 31:265–280. doi:10.1016/S0168-1699(00)00186-1

Bristow, K.L., G.J. Kluitenberg, and R. Horton. 1994a. Measurement of soil thermal properties with a dual-probe heat-pulse technique. Soil Sci. Soc. Am. J. 58:1288–1294. doi:10.2136/sssaj1994.03615995005800050002x

Bristow, K.L., R.D. White, and G.J. Kluitenberg. 1994b. Comparison of single and dual probes for measuring soil thermal properties with transient heating. Aust. J. Soil Res. 32:447–464. doi:10.1071/SR9940447

Campbell, D.I., C.E. Laybourne, and I.J. Blair. 2002. Measuring peat moisture content using the dual-probe heat pulse technique. Aust. J. Soil Res. 40:177–190. doi:10.1071/SR00108

Campbell, G.S., C. Calissendorff, and J.H. Williams. 1991. Probe for measuring soil specific heat using a heat-pulse method. Soil Sci. Soc. Am. J. 55:291–293. doi:10.2136/sssaj1991.03615995005500010052x

Chen, J., J.W. Hopmans, and M.E. Grismer. 1999. Parameter estimation of two-fluid capillary pressure–saturation and permeability functions. Adv. Water Resour. 22:479–493. doi:10.1016/S0309-1708(98)00025-6

de Vries, D.A., and A.J. Peck. 1958. On the cylindrical probe method of measuring thermal conductivity with special reference to soils: II. Analysis of moisture effects. Aust. J. Phys. 11:409–423. doi:10.1071/PH580409

Eching, S.O., J.W. Hopmans, and O. Wendroth. 1994. Unsaturated hydraulic conductivity from transient multistep outflow and soil water pressure data. Soil Sci. Soc. Am. J. 58:687–695. doi:10.2136/sssaj1994.03615995005800030008x

Ham, J.M., and E.J. Benson. 2004. On the construction and calibration of dual-probe heat capacity sensors. Soil Sci. Soc. Am. J. 68:1185–1190. doi:10.2136/sssaj2004.1185

Heitman, J.L., J.M. Basinger, G.J. Kluitenberg, J.M. Ham, J.M. Frank, and P.L. Barnes. 2003. Field evaluation of the dual-probe heat-pulse method for measuring soil water content. Vadose Zone J. 2:552–560. doi:10.2136/vzj2003.5520

Hopmans, J.W., J. Šimůnek, and K.L. Bristow. 2002. Indirect estimation of soil thermal properties and water flux using heat pulse probe measurements: Geometry and dispersion effects. Water Resour. Res. 38(1). doi:10.1029/2000WR000071

Kamai, T., G.J. Kluitenberg, and J.W. Hopmans. 2009. Design and numerical analysis of a button heat pulse probe for soil water content measurement. Vadose Zone J. 8:167–173. doi:10.2136/vzj2008.0106

Kamai, T., A. Tuli, G.J. Kluitenberg, and J.W. Hopmans. 2008. Soil water flux measurements near 1 cm d^{-1} using an improved heat pulse probe design. Water Resour. Res. 44:W00D14. doi:10.1029/2008WR007036

Kamai, T., A. Tuli, G.J. Kluitenberg, and J.W. Hopmans. 2010. Correction to "Soil water flux density measurements near 1 cm d^{-1} using an improved heat pulse probe design." Water Resour. Res. 46:W07901. doi:10.1029/2010WR009423

Kluitenberg, G.J. 2002. Heat capacity and specific heat. In: J.H. Dane and G.C. Topp, editors, Methods of soil analysis. Part 4. SSSA Book Ser. 5. SSSA, Madison, WI. p. 1201–1208. doi:10.2136/sssabookser5.4.c49

Kluitenberg, G.J., K.L. Bristow, and B.S. Das. 1995. Error analysis of heat pulse method for measuring soil heat capacity, diffusivity, and conductivity. Soil Sci. Soc. Am. J. 59:719–726. doi:10.2136/sssaj1995.03615995005900030013x

Kluitenberg, G.J., J.M. Ham, and K.L. Bristow. 1993. Error analysis of the heat pulse method for measuring soil volumetric heat capacity. Soil Sci. Soc. Am. J. 57:1444–1451. doi:10.2136/sssaj1993.03615995005700060008x

Kluitenberg, G.J., T. Kamai, J.A. Vrugt, and J.W. Hopmans. 2010. Effect of probe deflection on dual-probe heat-pulse thermal conductivity measurements. Soil Sci. Soc. Am. J. 74:1537–1540. doi:10.2136/sssaj2010.0016N

Knight, J.H., G.J. Kluitenberg, T. Kamai, and J.W. Hopmans. 2012. Semianalytical solution for dual-probe heat-pulse applications that accounts for probe radius and heat capacity. Vadose Zone J. 11(2). doi:10.2136/vzj2011.0112

Mori, Y., J.W. Hopmans, A.P. Mortensen, and G.J. Kluitenberg. 2003. Multi-functional heat pulse probe for the simultaneous measurement of soil water content, solute concentration, and heat transport parameters. Vadose Zone J. 2:561–571. doi:10.2136/vzj2003.5610

Ochsner, T.E., and J.M. Baker. 2008. In situ monitoring of soil thermal properties and heat flux during freezing and thawing. Soil Sci. Soc. Am. J. 72:1025–1032. doi:10.2136/sssaj2007.0283

Ochsner, T.E., R. Horton, G.J. Kluitenberg, and Q.J. Wang. 2005. Evaluation of the heat pulse ratio method for measuring soil water flux. Soil Sci. Soc. Am. J. 69:757–765. doi:10.2136/sssaj2004.0278

Ochsner, T.E., R. Horton, and T. Ren. 2003. Use of the dual-probe heat-pulse technique to monitor soil water content in the vadose zone. Vadose Zone J. 2:572–579. doi:10.2136/vzj2003.5720

Ochsner, T.E., R. Horton, and T.H. Ren. 2001. A new perspective on soil thermal properties. Soil Sci. Soc. Am. J. 65:1641–1647. doi:10.2136/sssaj2001.1641

Olmanson, O.K., and T.E. Ochsner. 2008. A partial cylindrical thermo-time domain reflectometry sensor. Soil Sci. Soc. Am. J. 72:571–577. doi:10.2136/sssaj2007.0084

Ren, T., K. Noborio, and R. Horton. 1999. Measuring soil water content, electrical conductivity, and thermal properties with a thermo-time domain reflectometry probe. Soil Sci. Soc. Am. J. 63:450–457. doi:10.2136/sssaj1999.03615995006300030005x

Ren, T., T.E. Ochsner, R. Horton, and Z. Ju. 2003. Heat-pulse method for soil water content measurement: Influence of the specific heat of the soil solids. Soil Sci. Soc. Am. J. 67:1631–1634. doi:10.2136/sssaj2003.1631

Song, Y., J.M. Ham, M.B. Kirkham, and G.J. Kluitenberg. 1998. Measuring soil water content under turfgrass using the dual-probe heat-pulse technique. J. Am. Soc. Hortic. Sci. 123:937–941.

Song, Y., M.B. Kirkham, J.M. Ham, and G.J. Kluitenberg. 1999. Dual probe heat pulse technique for measuring soil water content and sunflower water uptake. Soil Tillage Res. 50:345–348. doi:10.1016/S0167-1987(99)00014-8

Song, Y., M.B. Kirkham, J.M. Ham, and G.J. Kluitenberg. 2000. Root-zone hydraulic lift evaluated with the dual-probe heat-pulse technique. Aust. J. Soil Res. 38:927–935. doi:10.1071/SR99096

Stehfest, H. 1970a. Algorithm 368: Numerical inversion of Laplace transforms. Commun. ACM 13:47–49. doi:10.1145/361953.361969

Stehfest H. 1970b. Remark on Algorithm 368: Numerical inversion of Laplace transforms. Commun. ACM 13:624. doi:10.1145/355598.362787

Tarara, J.M., and J.M. Ham. 1997. Measuring soil water content in the laboratory and field with dual-probe heat-capacity sensors. Agron. J. 89:535–542. doi:10.2134/agronj1997.00021962008900040001x

Toride, N., M. Inoue, and F.J. Leij. 2003. Hydrodynamic dispersion in an unsaturated dune sand. Soil Sci. Soc. Am. J. 67:703–712. doi:10.2136/sssaj2003.0703

Welch, S.M., G.J. Kluitenberg, and K.L. Bristow. 1996. Rapid numerical estimation of soil thermal properties for a broad class of heat-pulse emitter geometries. Meas. Sci. Technol. 7:932–938. doi:10.1088/0957-0233/7/6/012